JAKARTA AND GREATER KUALA LUMPUR URBAN HEAT ISLAND DURING THE PANDEMIC OF COVID-19

Aditya SAPUTRA[1]*, Mohd Hairy bin IBRAHIM[2], Sharif Shofirun Sharif ALI[3], Christopher GOMEZ[4], Yuli PRIYANA[1], JUMADI[1], M. Iqbal Taufiqurrahman SUNARIYA[1], DANARDONO[1], Afif Ari WIBOWO[1], Agus Anggoro SIGIT[1], Choirul AMIN[1], Hamim Zaky HADIBASYIR[1], Kuswaji Dwi PRIYONO[1], Khusna FLUORIDA[5], Aditya SYAIFUDIN[5], Ridwan HAFIDZIN[6]

DOI: 10.21163/GT_2024.192.22

ABSTRACT

The Covid-19 outbreak rapidly became a global pandemic in December 2019, spreading through droplets, direct contact, and possibly airborne transmission. Southeast Asian nations like Malaysia and Indonesia experienced delayed outbreaks but saw a surge in cases. Analysing Covid-19 spatial patterns, especially concerning temperature and humidity, provides valuable insights. Utilizing remote sensing, allows studying the correlation between temperature conditions and Covid-19 outbreak patterns. This study focuses on investigating the impact of urban heat islands (UHIs) on Covid-19 outbreaks in Jakarta and Greater Kuala Lumpur, given their significant caseloads in Indonesia and Malaysia, respectively. The research integrates remote sensing, secondary data, and statistical analysis methods. Remote sensing was used to acquire land surface temperature (LST) and Normalized Difference Vegetation Index (NDVI). The analysis revealed that industrial and commercial areas were hotter than others during normal times, but during the pandemic, LST and UHI shifted from industrial to settlement areas due to large-scale social restrictions. This shift corresponded with the cessation of office, tourism, and industrial activities during lockdowns in March and July 2020 in Jakarta and Greater Kuala Lumpur, respectively. The concentration of people shifted from central business and industrial areas to residential areas during lockdowns, resulting in changes in UHI patterns.

Key-words: *LST, UHI, Covid 19, NDVI, Urban climate, Social restriction*

1. INTRODUCTION

In December 2019, the City of Wuhan which is located in Hubei, China developed into the epicentre of unknown pneumonia disease outbreaks. At the beginning, the number of the suspect increased both inside and outside China. At the same time, The China local government conducted rapid prevention to control the transmission of virus by conducting detail investigation of the virus, identification and insulated the positive suspect, continuous monitoring and medication the patient, also reconstruct the specific standard operational of patient diagnostic. As a result, at January 7, 2020, the China scientist successfully revealed the cause of unknown pneumonia outbreak in China. He found that the pneumonia was caused from a virus which later known as Corona Virus 2019 (Covid-19), (Heymann, 2020).

----

[1]*Geography Faculty, Universitas Muhammadiyah Surakarta, Indonesia; corresponding author* as105@ums.ac.id (AS), Yuli.Priyana@ums.ac.id (YP), Jumadi@ums.ac.id (J), iqbal.t.sunaria@ums.ac.id (ITS), dan115@ums.ac.id (D), aaw346@ums.ac.id (AAW), choirul.amin@ums.ac.id (CA), hamim.zaky.h@ums.ac.id (HZH), kdp130@ums.ac.id (KDP)

[2] *Dept. Geography and Envirnment, Human Sciences Faculty, Universiti Pendidikan Sultan Idris, Malaysia;* hairy@fsk.upsi.edu.my (MHI)

[3] *School of Government, College of Law, Government & International Studies (COLGIS), Universiti Utara Malaysia;* sshofirun@uum.edu.my (SSA)

[4] *Graduate Program of Maritime Science, Kobe University, Japan;* christophergomez@bear.kobe-u.ac.jp (CG)

[5] *Remote sensing and Geographic Information System Laboratory, Geography Faculty, Universitas Muhammadiyah Surakarta, Indonesia;* khusnaf@gmail.com (KF), aditya.saifuddin@mail.ugm.ac.id (ASN)

[6] *Regional Planning Laboratory, Geography Faculty, Universitas Muhammadiyah Surakarta, Indonesia;* ridwan.hafidzin@gmail.com (RH)

At early stage of pandemic, Covid-19 started to infect the other countries who has close relationship with China such as Thailand, Japan, Korea, USA, Vietnam dan Singapore (China National Commission, 2020). The suspect of Covid-19 increased both in China and other countries. More than ten of thousands positive cases associated with Covid-19 were identified in several countries. The Covid-19 spread rapidly through droplet, direct contact to the positive suspect, and was able to spread airborne (Luo and Gao, 2020; Lu, Stratton and Tang, 2020; Wang, Tang, and Wei, 2020; Li et al., 2020).

Malaysia and Indonesia are Southeast Asia Countries that experienced spread of Covid-19 on Late January and early March 2020, respectively. It was slightly different with the other four neighbouring countries such as Thailand, Vietnam, Singapore, and Australia which started the Covid-19 spread on December 2019. Similar with other countries, the number of infected Covid-19 in Indonesia and Malaysia increased exponentially at the beginning stage of pandemic. On April 2020, the accumulative positive cases of Covid-19 reached 5,780 people with the number of death around 98 people. Meanwhile, in Indonesia there were 7,125 positive cases of Covid-19 with the number of death around 616 people. The distribution of Covid-19 cases in Malaysia and Indonesia until April 2020 is provided in **Figure 1 and 2** below.

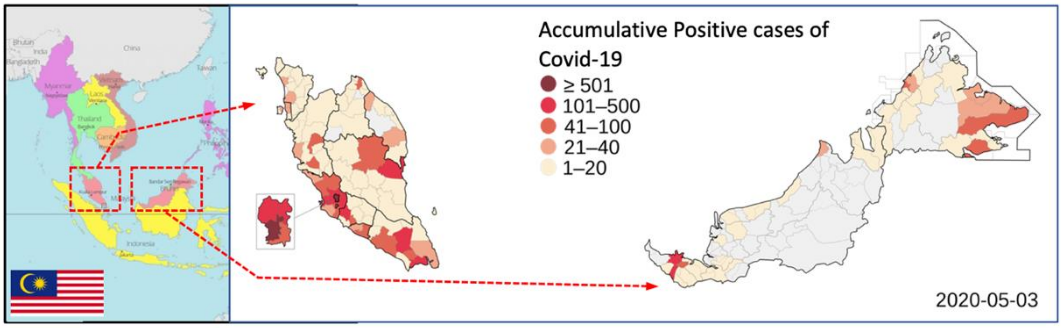

Fig. 1. The Covid-19 outbreak in Malaysia until 3 May 2020.
Source: Ministry of Health of Malaysia, 2020.
.

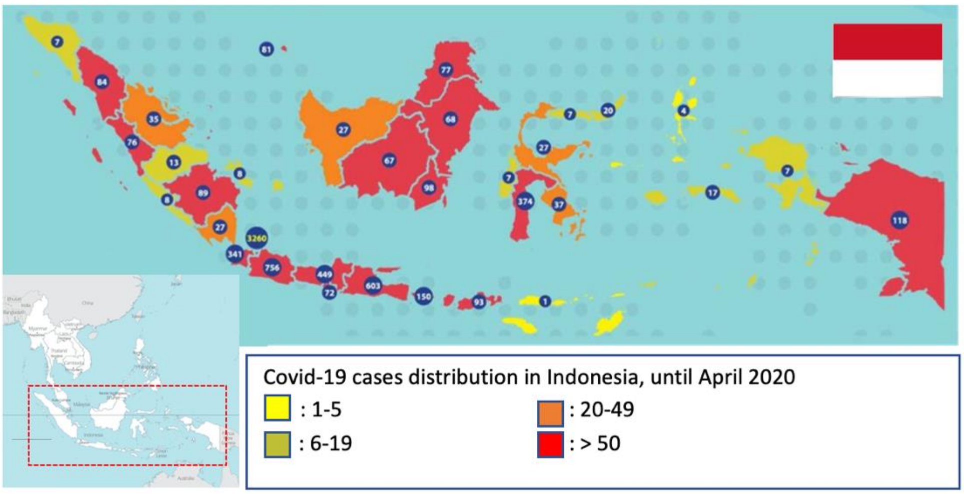

Fig. 2. Distribution of Covid-19 outbreaks in Indonesia until 20 April 2020.
Source: Badan Nasional Penanggulangan Bencana (BNPB)/ National Disaster Management Agency, Indonesia, 2020.

In term of spatial pattern of Covid-19 outbreaks, there were some interesting facts that need to be observed further. At the beginning of outbreaks (December 2019-January 2020), the Covid-19 infected the country which is located in the high latitude such as US (Naeger & Murphy, 2020; Dutta et al., 2021), Italy (Bassani et al., 2021) and France (Kovacs & Haidu, 2021; Kovacs & Haidu, 2022). Araujo and Naimi (2020) found that based on the mathematical model, tropical climate with the high temperature is able to unstable the virus and make it easy to die. Previous researches also concluded the similar things. The temperature and humidity level affect the level of virus transmission in particular area. Thus in high latitude countries (low temperature and low humidity), the virus grow and spread rapidly across the country (Chen et al., 2020, Sajadi et al. 2020; Sun et al. 2020; dan Wang et al. 2020). The cold air temperature and low humidity condition are evidently helps the virus to last longer (Sun et al., 2020). Based on the spatial pattern analysis, the area with average surface temperature 5.810C and minimum-maximum temperature of -3.440C – 12.550C are closely associated with the location of Covid-19 infected people.

Indonesia and Malaysia which is located in tropical area have relatively high temperature and humidity comparing the other high latitude countries. Thus this condition can reduce the rate of the virus outbreaks. Based on the climate monitoring, in general, the temperature and humidity level in Indonesia and Malaysia increase in April to August 2020. However, the Covid-19 transmission still occur in several big cities in Indonesia and Malaysia such as Jakarta and Kuala Lumpur. Thus this phenomena need to be further observed to get the better understanding how far the climate element (temperature and humidity) inhibit the rate of virus outbreaks.

The temperature information can be easily obtained from remote sensing technology. Without any direct contact into research area, the temperature and humidity level can be precisely discovered. One of the satellite imageries that can be used to extract the temperature data is Landsat 8 OLI (Prohmdirek et al., 2020). Landsat provide 11 bands with 2 channels (10 and 11) which consists the thermal infrared (TIR). These channels able to record the surface temperature of the observed object. Thus it will interesting to conduct a research about the spatial analysis of relationship between temperature condition and the Covid-19 outbreak pattern. The urban heat island (UHI) will used as main parameter to characterise the temperature and humidity condition in Jakarta and Greater Kuala Lumpur. By identify the UHI pattern, the local temperature which affected by land use and air pollution can be identified accurately (Ibrahim, 2019). Thus, based on the aforementioned background above, this study aims to understand the urban heat island during the Covid-19 outbreak. Two big cities, The Greater Jakarta and Greater Kuala Lumpur, were chosen to conduct this research. In term of the number of the confirmed positive cases, both cities have the largest number of confirmed positive cases in Indonesia and Malaysia.

2. STUDY AREA

The two largest cities in Southeast Asia, Jakarta and Greater Kuala Lumpur, are presented in a comparative analysis in the present study. Those two cities is similar in terms of physical and human geography, the growth with respect to population size are in contrast to each other. Jakarta has around 9.61 million population, while Kuala Lumpur only 1.63 million population. Jakarta, is coastal city located in the north cost of west part of Java. Jakarta is the capital city of Indonesia and, therefore, is a centre of a large number of executive buildings and residential areas. Similar with Jakarta, Kuala Lumpur, is a coastal city and is the financial capital of the country. Kuala Lumpur located in the west coast of Malaysia close to the busiest strait in the world namely Malaka Strait. Gemorphologically, Kuala Lumpur is characterised as a huge valley known as “*Lembah Klang*” or Klang Valley which bordered by Titiwangsa mountainous area in the east, north and south and also bordered by the Malaka Strait in the west.

Jakarta expands into a Jakarta Metropolitan Region (JMR) or known as Jabodetabek (Jakarta-Bogor-Depok-Tangerang-Bekasi). This area develop into urban area which support the activities in the Jakarta as capitol city Indonesia. This area covers the sub-urban area in the west (Tangerang), south (Bogor and Depok), and the east (Bekasi) (Taki and Maatouk, 2018). Similar with Jakarta, Kuala Lumpur expand rapidly to the east side (Hulu Langat) and north (Gombak) of the city (Boori et al., 2015). The west and the south side of the City Centre Commercial (CCC) Kuala Lumpur is bordered with the busy industrial area known as Petaling Jaya and Putra Jaya, respectively. There are also two important public facilities which are located in Petaling jaya and Putra Jaya, i.e., Klang Seaport in Petaling Jaya and international airport Kuala Lumpur in Putra Jaya. Kuala Lumpur also expand rapidly into Greater Kuala Lumpur which consists of Sabak Bernam, Kuala Selangor, Ulu Selangor and Gombak in the north part; Klang and Petaling in the west part; Kuala Langat and Sepang in the south part; and Ulu Langat in the east part of Kuala Lumpur City Centre,

In term of climate, Jakarta and Greater Kuala Lumpur has similar tropical climate. The average monthly temperature are between 26 to 28^{0}C (Masoudi et al., 2019). Both Jakarta and Greater Kuala Lumpur has dry and rainy season which affected by the monsoonal wind. **Figure 3** below shows that the Jakarta and Greater Kuala Lumpur have similar pattern of temperature, monthly average rainfall, humidity and daylight, because they are located in the same climatic zone and greatly influenced by the ocean (**Fig. 4**).

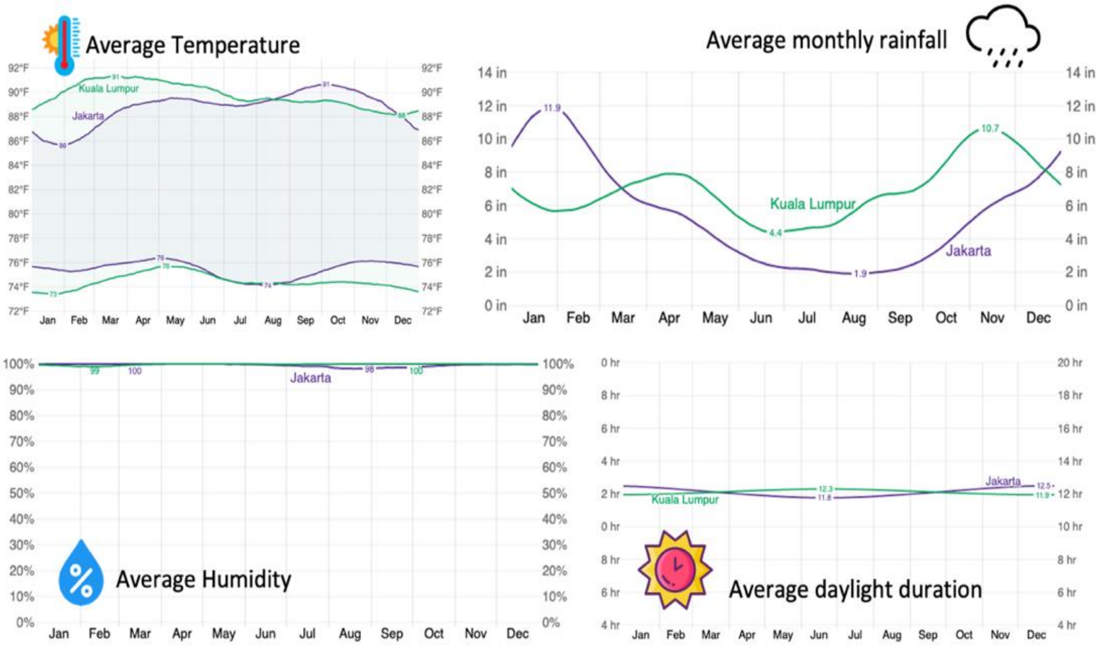

Fig. 3. Comparison of monthly average temperature, monthly rainfall, humidity, and daylight duration in Jakarta and Kuala Lumpur.

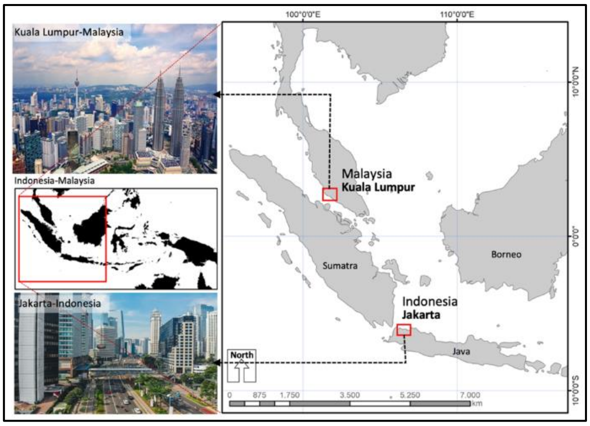

Fig. 4. Jakarta and Greater Kuala Lumpur map.

3. DATA AND METHODS

There are three main steps to conduct this study, first step is to know the covid-19 distribution in study area (Jakarta-Kuala Lumpur). The second step is two extract the surface temperature and the third step are to calculate the Urban Heat Island (UHI). The last step is to analyse the relationship between covid-19 distribution and UHI index. The LST will be extracted by using several equations through remote sensing software based on the image analysis of Landsat 8 OLI (Worachairungreung et al., 2023). Landsat 8 OLI or often called as L8 is the newest generation of Landsat after Landsat 7 ETM was stated experienced damage on one of the scanner sensors especially on Scan Line Corrector (SLC) on May 2003. Since that time, L8 was launched to work around 5 year. The main objective of L8 is to continue providing data which had been done by the previous generation. This project (L8) provides the satellite imagery which has faster temporal resolution (16 days) and also provides an open-source image base on the cloud platform. L8 carries several new innovations from the previous generation. The comparison between Landsat 7 and 8 can be seen in **Table 1**. The L8 was designed to have Sun-Synchronous with the altitude of 705 km. L8 has 16 days of temporal resolution with 98.9 minutes of orbital time travel. L8 carries 2 main sensors namely OLI and TIRS. OLI was made by BATC and TIRS was developed by NASA GSFC. Both of them have ability to records simultaneously, although they can operate individually if damage occurs on one of the sensors. Furthermore, there are also slightly different in term of the number of carried bands. The detail information of bands in Landsat 7 and 8 can be seen in **Table 2**.

Table 1.

The observation ability in L7 and L8.

	Landsat 7	**Landsat 8**
Scene per day	~450	~700
SSR size	378 Gbits, Block-based	3.14 Terabit, file-based
Type of Sensor	ETM+, Whisk-Broom	OLI/ TIRS, Push broom
Compression	No	~2:1 Variable rice compression
Data rate	150 Mbits/ second x 3 bands/ frequency	384 Mbits/ second, CCSDS bands virtual
Encoding	No all of CCSDS compliant	CCSDS, LDPC FEC
Range	S-band 2-way Droppler	GPS
Orbit	705 km Sun-syn. $98,2^0$	705 km Sun-syn. $98,2^0$
Crossing time	~10:00 AM ± 15 minutes	~10:00 AM ± 15 minutes

Source: USGS, 2019.

Table 2.

Comparison of bands between Landsat 7 and 8.

Bands (μm) of Landsat 7 ETM+			**Bands (μm) of Landsat 8 OLI and TIRS**		
			30 m Coastal/ Aerosol	0,435-0,451	Band 1
Band 1	30 m Blue	0,441-0,514	30 m Blue	0,452-0,512	Band 2
Band 2	30 m Green	0,519-0,601	30 m Green	0,533-0,590	Band 3
Band 3	30 m Red	0,631-0,692	30 m Red	0,636-0,673	Band 4
Band 4	30 m NIR	0,772-0,898	30 m NIR	0,851-0,879	Band 5
Band 5	30 m SWIR-1	1,547-1,749	30 m SWIR-1	1,566-1,651	Band 6
Band 6	60 m TIR	10,31-12,36	100 m TIR-1	10.60-11.91	Band 10
			100 m TIR-2	11.50-12.51	Band 11
Band 7	30 m SWIR-2	2,064-2,345	30 m SWIR-2	2,107-2,294	Band 7
Band 8	15 m Pan	0,515-0,896	15 m Pan	0,503-0,676	Band 8
			30 m Cirrus	1.363-1.384	Band 9

Source: USGS, 2019.

Urban Heat Island (UHI) can be defined as the urban temperature transformation in comparison to their surroundings area (Schwarz et al. 2011). Two common approaches to calculate the UHI are first, direct air temperature measurement, and second, measuring the surface temperature (Streutker, 2003). Today with the rapid enhancement of remote sensing technology, the land surface temperature can be obtained through satellite imagery analysis to support the UHI study around the globe. Several studies in different type of satellite imagery had been conducted to obtain the land surface temperature in order to support the UHI study. Schwarz et al. (2011), Tomlinson et al. (2012) and Miao et al. (2009), succeeded to extract the land surface temperature and to analyse the UHI through low-resolution sensor (MODIS). Meanwhile Chen et al. (2006), Zha et al. (2003), Liu & Zhang (2011) and Kaplan et al (2018), successfully utilized the middle resolution image such as Landsat 8 OLI and ASTER to study the UHI for particular cities and smaller area. Most of those previous study revealed that the different level of UHI is dominantly controlled by surface temperature which depends on the function of different land cover (Owen et al., 1998) especially the vegetation abundance (Chen et al., 2006; Gallo and Owen, 1999; Weng, 2001; and Weng et al., 2004). The recent study analysis the UHI phenomena during the pandemic Covid in two similar areas, i.e. greater Kuala Lumpur, Malaysia and Jakarta, Indonesia. Both areas are compared the UHI before and during the pandemic COVID-19. LANDSAT-8 on May, July, September, and December 2020 were used to obtain the LST and UHI. Meanwhile, Landsat 8 on March and August 2019 and 2020 were used to generate LST and UHI in Greater Kuala Lumpur. This recent study analysed also the relationship between the policy during the pandemic covid 19 and the UHI pattern.

In Malaysia, Covid-19 case started on Januari 25, 2020 (Hashim et al., 2021) and the government applied Lockdown in mid-March (Yusof, 2021). Meanwhile, In Indonesia first case of COVID-19 started on March 2, 2020 (Damaledo, 2021) and first lockdown in Indonesia as known as PSBB (Large-Scale Social Restrictions) which was applied in April 10, 2020. The data used represented 2 season, dry season and wet season in Jakarta and Kuala Lumpur. The data used is the Landsat 8 OLI with minimum cloud cover. The UHI identification consist of several steps such as calculating the radiance value of the satellite imagery, brightness temperature value conversion, and calculating the Land Surface Emissivity (LSE). The LSE was calculated by considering the Normalized Difference Vegetation Index (NDVI) and Proportion of Vegetation (PV) (Sobrino et al., 2004). The set of equation was used to generate the UHI index and the research flow can be seen in **Figure 5**.

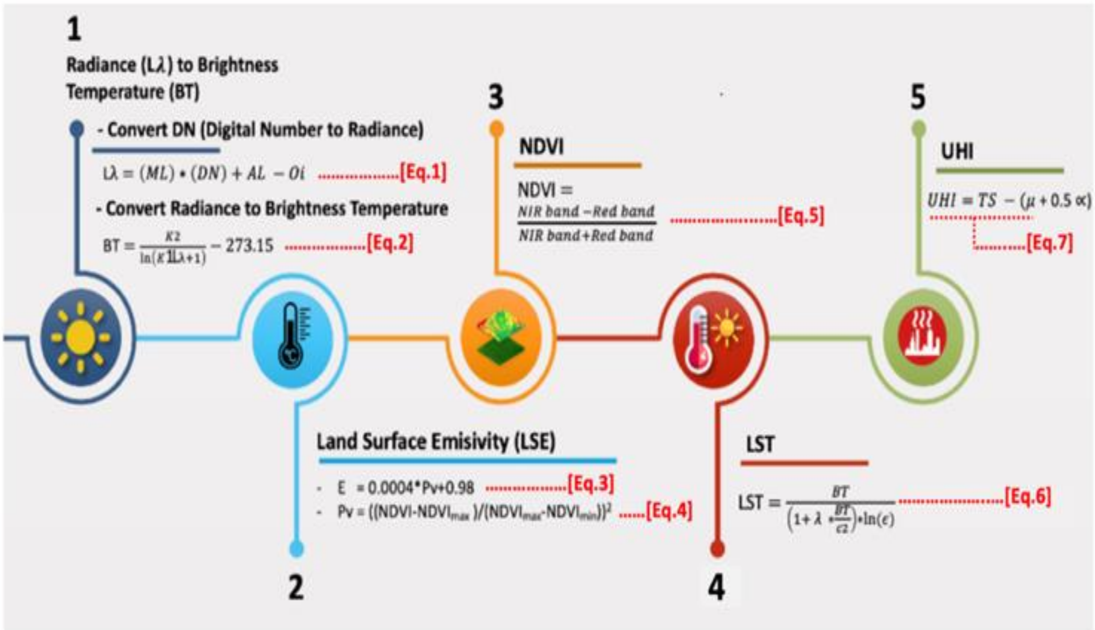

Fig. 5. The workflow of the research.

Note. *$L\lambda$: Radiance; ML and AL: factor value radiance from metadata; DN: digital number of each pixels; BT: Brightness Temperature; K1 and K2: Obtain from metadata of Landsat imagery is constant value; E: Emissivity; Pv: proportion vegetation value; NDVI: Normalised different Vegetation Index; LST: land surface temperature; C2 follow equation 7 below; UHI is urban heat island; TS is land surface temperature, μ is the average value of TS and α is standard deviation of TS.*

Equation 7.

$$C2 = h\frac{c}{s}$$

h = Planck constant value (1.38 x 10^{-23} JK^{-1}); c is light speed vacuum (2,998 X 10-8 $^{Ms-1}$); s = Boltzmann constant value (1.38 x 10^{-23} JK^{-1}); C2 value is constant around 14,338 MK.

4. RESULTS

4.1. Land surface temperature (LST)

Air temperature and surface temperature is slightly different. Air temperature refers to the measurement of the temperature of the air in the Earth's atmosphere. It is typically measured at a certain height above the ground, often at around 1.5 to 2 meters (5 to 6.5 feet) above the surface. This measurement is commonly recorded using thermometers placed inside a weather station or other measuring devices. Air temperature is an important parameter in weather forecasting, climate studies, and various applications ranging from agriculture to energy consumption predictions. It plays a significant role in determining weather patterns, as variations in air temperature lead to changes in atmospheric pressure, wind patterns, and precipitation. (Good et al., 2017). Land surface temperature (LST) refers to the temperature of the actual land or ground surface itself. LST can be vary based on the factors such as land cover (forests, urban areas, deserts), moisture content, and solar radiation received by the surface. LST is commonly measured using remote sensing techniques, such as satellite sensors that detect infrared radiation emitted by the Earth's surface. These sensors can provide a comprehensive view of land surface temperatures across large geographic areas. LST data are crucial for studying urban heat islands, monitoring agricultural productivity, assessing environmental changes, and understanding the Earth's energy balance.

During the observation months (May, July, September and December 2020), there are strong heterogeneity of land surface temperature in Jakarta. The observed months refers to the dry and wet season in Indonesia. July-September represent the wet season, meanwhile December represent the wet season. The land surface temperature variation also occur in different type of land cover over the Jakarta. The minimum surface temperature in the observed month are 13.42^{0}C, meanwhile, the highest surface temperature of study area is 35,73^{o}C. During the dry season which has low humidity and rainfall, the temperature near surface is vary between 13-34^{0}C. Meanwhile, the rainy season which has high humidity and rainfall, the temperature near surface is vary between 13-35^{0}C. The LST condition during the observation months can be seen in **Figure 6** below.

During the Pandemic Covid-19 LST in Greater Kuala Lumpur has similar pattern in Jakarta, Indonesia. There was a shift in LST distribution from industrial area (Pelabuhan Klang-Petaling Jaya) to settlement area in the east such as Wangsa Maju, Cheras, Hulu Langat and Puchong. In March 2020 (dry season), the LST in Kuala Lumpur range between 13.01 – 33.53^{0}C. The hot temperature tends to distribute in industrial area in Centre part of Greater Kuala Lumpur from west side (Klang) to the east part of Hulu Langat. In general, the centre to south part of Greater Kuala Lumpur experienced higher LST comparing than the north part of Kuala Lumpur (**Fig. 7** (left)). Whereas, LST in Greater Kuala Lumpur slightly shifted to the west direction during the August 2020. The LST value in August 2020 range between 15.92-35.48^{0}C.

The shifting LST mostly occurs because wind speed (Klysik & Fortuniak, 1999; Steeneveld et al., 2011; Wang et al., 2019), or water index variability (Binarti & Santoso, 2023). However, recently during the covid-19 pandemic, the population restriction policy indirectly affects the LST pattern (Hadibasyir et al., 2020; Saputra et al., 2022). The restriction policy forced the people to stay and work at home to decrease the covid-19 transmission. As a results, the LST pattern move to the settlement area due to high energy and electricity consumption in household level (Shofirun et al., 2023; Elvidge et al., 1997; Bessec et al., 2008).

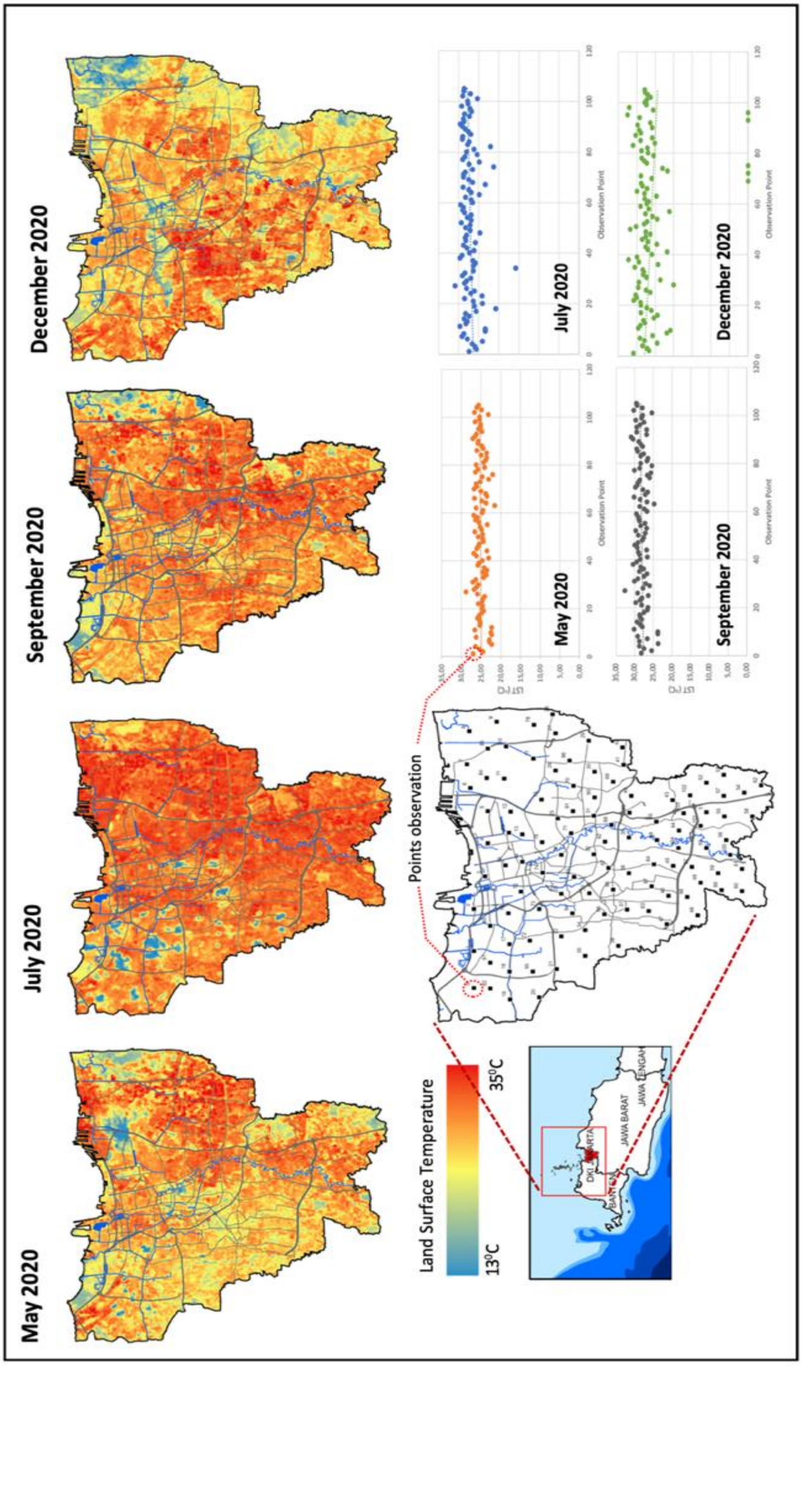

Fig. 6. The LST in Jakarta during May, July, September and December 2020.

The LST pattern in March and August 2020 can be seen in **Figure 7** (Left) and 7(Right) below.

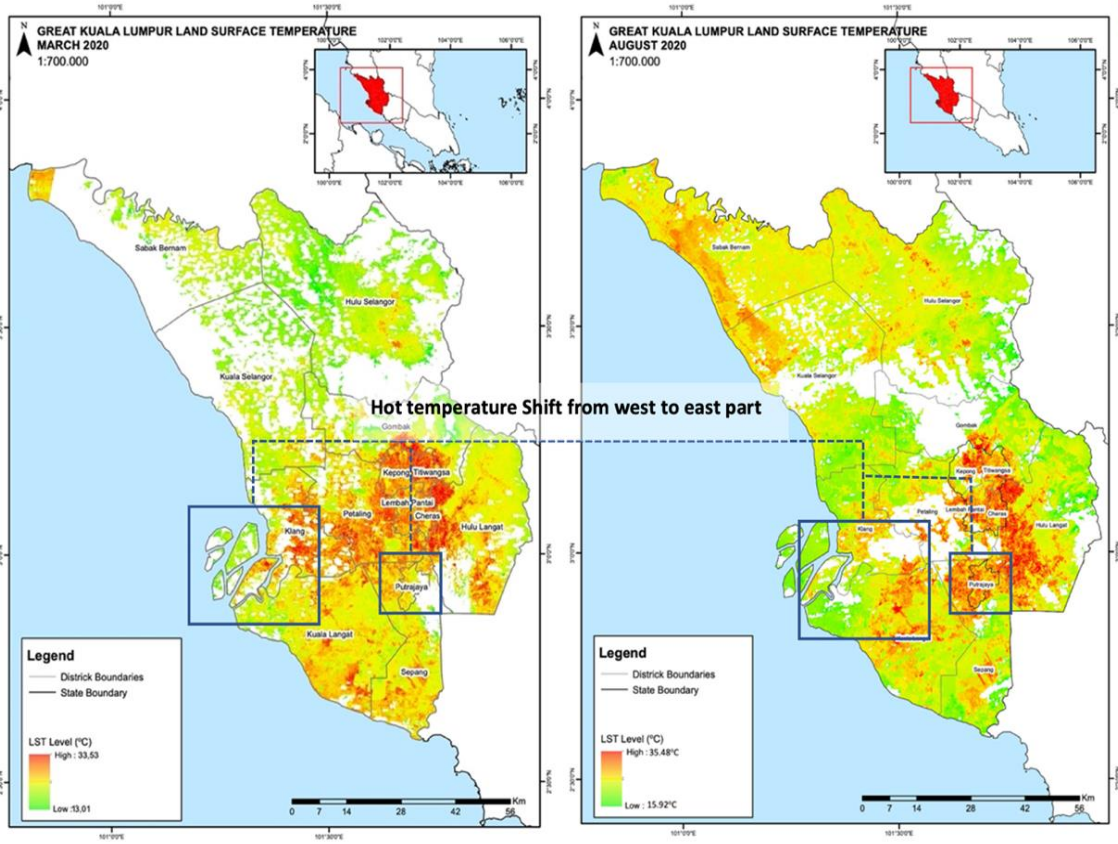

Fig. 7. LST Greater Kuala Lumpur in March 2020 (left) and August 2020 (right).

4.2. Urban Heat Island (UHI)

The phenomenon where a particular area has a higher temperature compared to its surroundings is known as the urban heat island effect. In the most of big cities, the temperature at the city centre is observed to be elevated in comparison to the surrounding areas (Adinna et al. 2009; Synnefa et al. 2008; Yamamoto 2006). In general, Jakarta and Greater Kuala Lumpur have similar pattern of UHI phenomena. In Jakarta, UHI tend to occurs in industrial area which are located in the north and east part of Jakarta. While, in Greater Kuala Lumpur UHI tend to occur in city centre (Central Part) and industrial area (west part). The value of UHI in Jakarta range between 0-5.8ºC and 0-7.7ºC in July and December 2020, respectively. On the other hand, The UHI in Greater Kuala Lumpur range between 0-9.5ºC and 0-11.3ºC in March and August 2020, respectively. The UHI distribution both In Jakarta and Greater Kuala Lumpur is provided in **Figure 8** below.

5. DISCUSSION

During pandemic of Covid-19 every country has their own regulation to minimise the virus transmission and fatalities. Jakarta, capitol city of Indonesia, implemented several policies to reduce the virus transmission. Jakarta at least implemented 5 large-scale social restriction (PSBB) in May-December 2020 and Activities Restriction Enforcement (PPKM) in January to December 2021. The PSBB including work from home, social distancing, restriction on public and sociocultural event or services and limitation of public transportation (Retnowati et al., 2022).

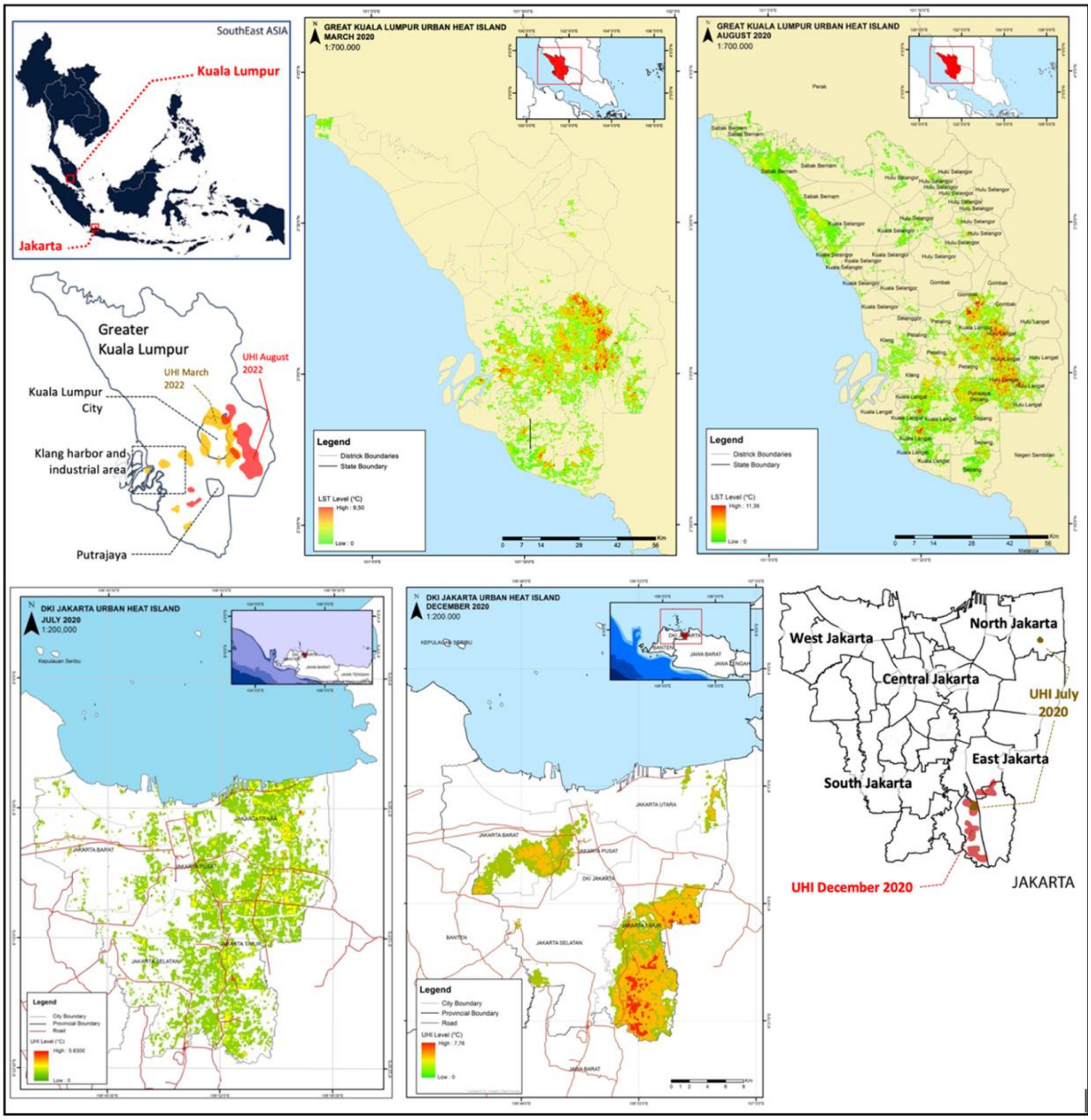

Fig. 8. UHI distribution in Kuala Lumpur (above) in March 2020 (left) and August 2020 (right); UHI distribution in Jakarta (below) in July 2020 (left) and December 2020 (right).

PSBB allows only important sector such as health facility, food, and banking to keep open with certain rule. Meanwhile, PPKM regulates the portion of Work from home (WFH) and work from office (WFO) also dine-in in the restaurant regulation (25% from capacity). By implementing these policies, Indonesia government succeeded to reduce the virus transmission. Furthermore, this policy also indirectly affects the LST and UHI pattern. In July 2020 when Jakarta implemented the PSBB Stage, the UHI condition has the ordinary pattern. The UHI occurred in city center, CBD, industrial area and commercial area. However, in December 2020 when the Jakarta implemented PSBB stage 5, the UHI shifted form commercial, CBD, city center and industrial area to settlement area in the East and West Jakarta. The reason for this lies in the fact that the rigorous policy endorsed limitations on social activities, encompassing office tasks, entertainment, and public transportation. As a result, the people most spend their time at home and caused more consumption on energy and electricity. This accumulation condition will lead to increase the air and surface temperature.

Similar to Jakarta, The UHI in Greater Kuala Lumpur were shifted as some social regulations applied during the pandemic Covid-19. During the pandemic Covid-19 Malaysia government applied at least 6 phases of Social Restriction namely Pre-Movement Control Order (Pre-MCO), MCO, Conditional MCO, Recovery MCO, Extended MCO, and MCO 2.0. (Rajendran, 2021) (**Fig. 10**). Full lockdown or MCO were applied in early stage of pandemic, 18 March-3 May 2020. All sectors were lockdown except important sector such health, food supply, bank, and logistics. As a results some industrial and commercial area such Klang Harbour and industrial areas and Kuala Lumpur City Centre (KLCC) were closed. This condition effect the UHI pattern in Greater Kuala Lumpur. UHI tend to arise in settlement area eastern part of KLCC (**Fig. 8**). This results in line with the previous research (Shofirun et al., 2023; Elvidge et al., 1997; Bessec et al., 2008; Hadibasyir et al., 2020) who found that social restriction policy forced the people to limit their movement and keep stay at home. Thus, when somebody stay longer in the home means the energy and electricity consumption also increase. This prolonged situation will lead the LST as well as UHI in the atmosphere. The detail illustration of the relationship between the applied social regulation during pandemic, covid-19 cases, air temperature, and UHI in Jakarta and Greater Kuala Lumpur can be seen in **Figure 9 and 10**, respectively.

The shifting pattern of UHI was also signified when the UHI in the same months a year before Covid-19 compared with the UHI during the pandemic. For instance, in Greater Kuala Lumpur, the UHI of March and August 2019 (normal condition, before Covid-19) occurred in the Klang Harbour and Industrial area in March and August 2019. During the Covid-19, when the government applied the Pre-MCO and RMCO (March and August 2020) the UHI shifted to the settlement area in the east part of KLCC. The Greater Kuala Lumpur UHI shifting before and during the pandemic can be seen in **Figure 11**.

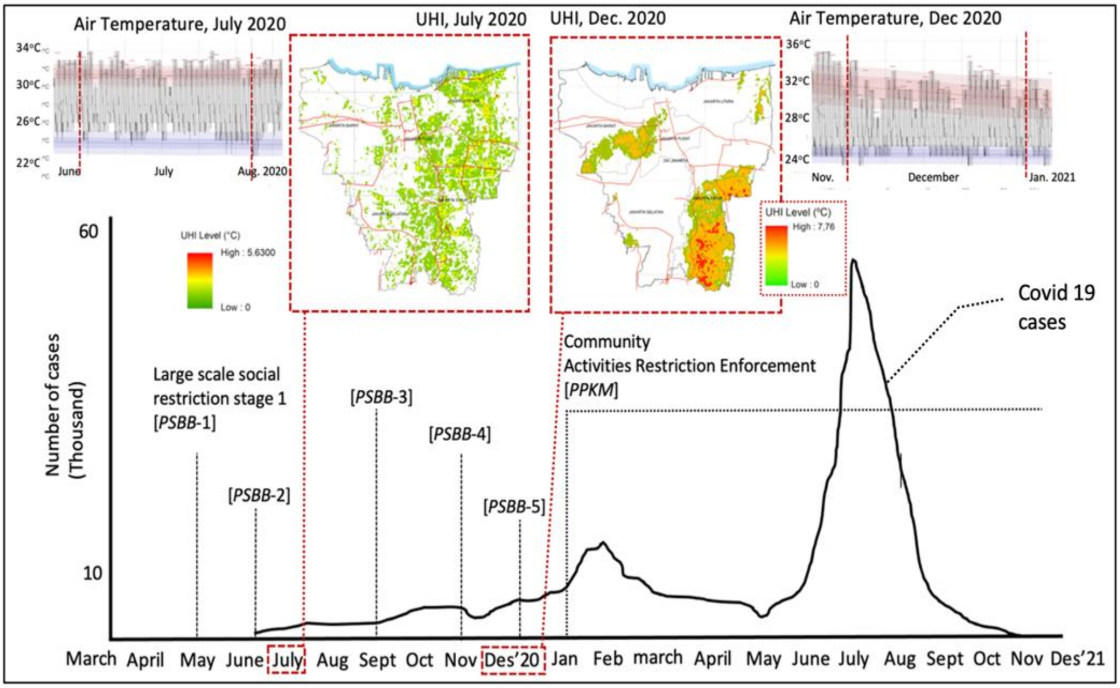

Fig. 9. Covid-19 cases, applied regulation, UHI and air temperature in Jakarta.

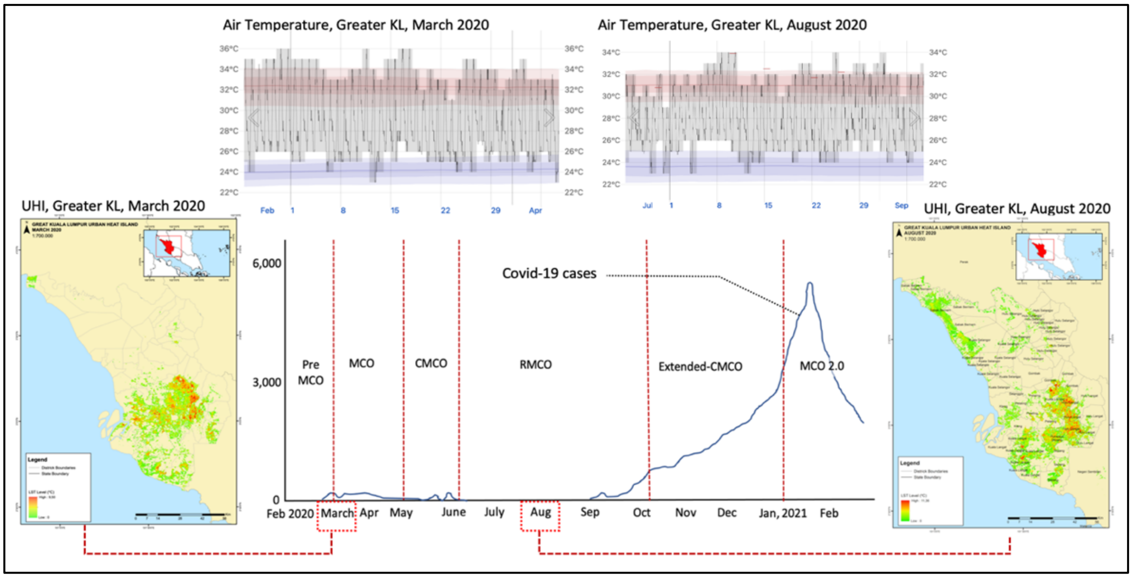

Fig. 10. Covid-19 cases, applied regulation, UHI and air temperature in Greater Kuala Lumpur, March and August 2020.

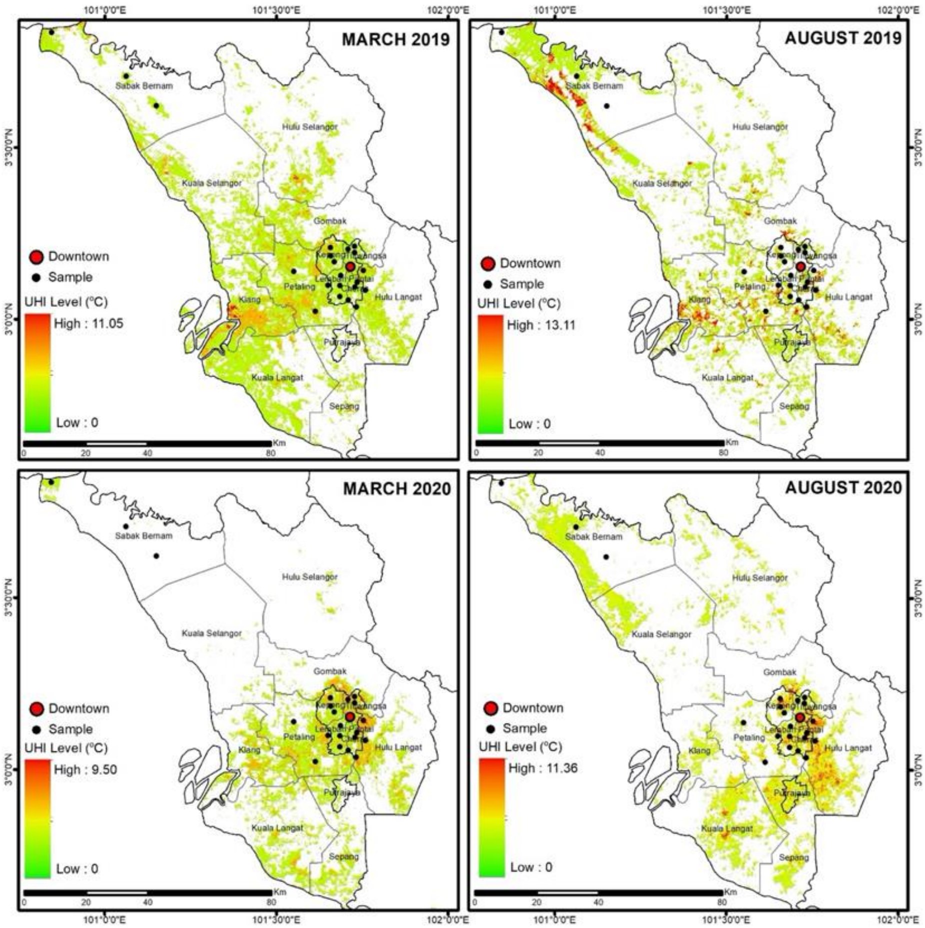

Fig. 11. UHI shifting in Greater Kuala Lumpur before and during the pandemic.

6. CONCLUSIONS

This study has compared the LST and UHI pattern between different social regulation during pandemic Covid-19 both in Jakarta and Greater Kuala Lumpur. Results showed that the LST and UHI has shifted during the two observed months (July-December 2020 in Jakarta and March-August 2020 in Greater Kuala Lumpur). In July and December 2020, the Indonesian government applied large scale social restriction (PSBB) stage 2 and stage 5, respectively. The government policy forced the population to stay at home. Thus, further this condition affected the LST and UHI pattern. Results showed that during the observed month the LST and UHI shifted from industrial area to settlement area.

Similar to Jakarta, Greater Kuala Lumpur has experienced the same LST and UHI movement. During the observed month March 2020, Kuala Lumpur experienced by transition regulation from pre MCO to fully MCO, meanwhile in December 2020 Malaysian Government applied Recovery MCO (RMCO). As a results, the LST and UHI started to decrease in Industrial area and appeared in settlement area in the east part of KLCC in March 2020 and in December 2020, the LST and UHI occurred in majority settlement area in the east part of Kuala Lumpur due to the RMCO regulation.

R E F E R E N C E S

Adinna, E., Christian, E. I., and Okolie, A. T. (2009). Assessment of urban heat island and possible adaptations in Enugu urban using Landsat-ETM. *Journal of Geography and Regional Planning*, **2**(2), 030-036.

Araujo, MB. & Naimi, B. (2020). Spread of SARS-CoV-2 Coronavirus likely constrained by climate. medRxiv; DOI: 10.1101/2020.03.12.20034728.

Bassani, C., Vichi, F., Esposito, G., Montagnoli, M., Giusto, M., & Ianniello, A. (2021). Nitrogen dioxide reductions from satellite and surface observations during COVID-19 mitigation in Rome (Italy). *Environmental Science and Pollution Research*, **28**, 22981-23004. https://doi.org/10.1007/s11356-020-12141-9

Bessec, M. & Fouquau, J. (2008). The Non-linear Link between Electricity Consumption and Temperature in Europe: A Threshold Panel Approach. *Energy Economics*, **30**(5), 2705–2721.

Binarti, F. & Santoso, A.J. (2023). Identifying climate change vulnerability based on land cover indicators: a case study in Surabaya, Indonesia. *Geographia Technica*, **18**(1), 71-84. http://dx.doi.org/10.21163/GT_2023.181.06

Boori, M.S., Netzband, M., Coudhary, K., Vozenilek, V. (2015). Monitoring and modeling of urban sprawl through remote sensing and GIS in Kuala Lumpur, Malaysia. *Ecological Processes*, **4**(1). DOI: 10.1186/s13717-015-0040-2

Chen, X-L., Zhao, H.-M., Li, P.-X., Yin, Z.-Y. (2006). Remote sensing image -based analysis of the relationship between urban heat island and land use/cover changes. *Remote Sensing Environment*, **104**. 133-146.

Cina National Health Commission. (2020) Update on the novel coronavirus pneumonia outbreak (Jan 24, 2020). Beijing: Cina National Health Commission. http://www.nhc.gov.cn/xcs/yqdt/202001/c5da49c4c5bf4bc320ec2036480627.shml (accessed Jan 24, 2020)

Damaledo, Y. D. (2021). Kasus Corona Pertama di Indonesia Diumumkan Tahun Lalu [Kesehatan]. Tirto.Id. https://tirto.id/2-maret-2020-kasus-corona-pertama-di-indonesia-diumumkan-tahun-lalu-gaKw

Dutta, V., Kumar, S., & Dubey, D. (2021). Recent advances in satellite mapping of global air quality: evidences during COVID-19 pandemic. *Environmental Sustainability*, **4**(3), 469-487. https://doi.org/10.1007/s42398-021-00166-w

Elvidge, CD., Baugh, KE, Kihn, EA., Kroehl, HW., Davis, ER., and Davis, CW. (1997). Relation between Satellite Observed Visible-near Infrared Emissions, Population, Economic Activity and Electric Power Consumption. *International Journal of Remote Sensing*, **18**(6), 1373–1379.

Gallo, K.P., Owen, T.W. (1999) Satellite-based adjustment for the urban heat island temperature bias. *Journal Applied Meteorology*, **38**, 806-813.

Good, EJ., Ghent, DJ., Bulgin, CE., Remidios, JJ. (2017). A spatiotemporal analysis of the relationship between near-surface air temperature and satellite land surface temperatures using 17 years of data from the ATSR series. *JGR: Atmospheres*, **122**(17). https://doi.org/10.1002/2017JD026880

Hadibasyir, HZ., Rijal, SS. and Sari, DR. (2020). Comparison of Land Surface Temperature During and Before The Emergence of Covid-19 Using Modis Imagery in Wuhan City, *Forum Geogr*., **34**, 1–15.

Hashim JH, Adman MA, Hashim Z, Mohd Radi MF and Kwan SC (2021) COVID-19 Epidemic in Malaysia: Epidemic Progression, Challenges, and Response. *Front. Public Health* 9:560592. doi: 10.3389/fpubh.2021.560592

Heymann, D.L., (2020). A novel coronavirus outbreak of global health concern. *Thelancet*, **395**, 497-514. doi.org/10.1016/ S0140-6736(20)30185-9.

Ibrahim, S. & Halounova, L. (2019). Statistical study of MODIS algorithms in estimating aerosol optical depth over the Czech Republic. *Stavební Obzor - Civil Engineering Journal*, **28**(4), 523-531. https://doi.org/10.14311/CEJ.2019.04.0043

Kovacs, K. D. & Haidu, I. (2021). Effect of anti-COVID-19 measures on atmospheric pollutants correlated with the economies of medium-sized cities in 10 urban areas of Grand Est region, France. *Sustainable Cities and Society*, 74, 103173. https://doi.org/10.1016/j.scs.2021.103173

Kovács K.D. & Haidu I. (2022), Tracing out the effect of transportation infrastructure on NO2 concentration levels with Kernel Density Estimation by investigating successive COVID-19-induced lockdowns. *Environmental Pollution*, **309** : 119719. https://doi.org/10.1016/j.envpol.2022.119719

Li XG, Zai JJ, Wang XM, Li Y, (2020). Potential of large 'first generation' human-to-human transmission of 2019-nCoV. *J Med Virol*. https://doi.org/10.1002/jmv.25693

Liu, L and Zhang, Y. (2003). Urban heat island analysis using the Landsat TM and ASTER data: A case study in Hong Kong, *Remote Sensing*, **3**, 1535-1552

Luo G, Gao S-J. (2020). Global health concerns stirred by emerging viral infections. J Med Virol. 2020;92:399–400. https://doi.org/10.1002/jmv.25683

Lu H, Stratton CW, Tang YW. (2020). Outbreak of pneumonia of unknown ethology in Wuhan China: the mystery and the miracle. *J Med Virol*. https://doi.org/10.1002/jmv.25678

Kaplan, G., Avdan, U., Avdan, Z. Y. (2018) Urban heat island analysis using the Landsat 8 satellite data: A case study in Skopje, Macedonia. *MDPI Proceeding of 2nd International Electronic Conference of Remote Sensing*, 22 March-5 April 2018. 358, doi: 10.3990/ecrs-2-05171.

Kłysik, K., and Fortuniak, K. (1999). Temporal and spatial characteristics of the urban heat island of Ło´ dz´ , Poland, Atmos. Environ. 33 (24– 25) (1999) 3885–3895

Masoudi, M., Tan, P. Y., & Liew, S. C. (2019). Multi-city comparison of the relationships between spatial pattern and cooling effect of urban green spaces in four major Asian cities. *Ecological Indicators*, **98**, 200–213. Doi: 10.1016/j.ecolind.2018.09.058

Miao, S., Chen, F., LeMone, M.A., Tewari, M., Li, Q., Wang, Y. (2009). An observational and modeling study of characteristics of urban heat island and boundary layer structures in Beijing. *Journal Applied Meteorology and Climatology*, **48**, 484-501.

Naeger, A. R., & Murphy, K. (2020). Impact of COVID-19 containment measures on air pollution in California. *Aerosol and Air Quality Research*, **20**(10), 2025-2034. https://doi.org/10.4209/aaqr.2020.05.0227

Owen, T., Carlson, T., Gillies, R. (1998) An assessment of satellite remotely-sensed land cover parameter in quantitatively describing the climatic effect of urbanization. *International Journal of Remote Sensing*. **19**, 1663-1681.

Prohmdirek, T., Chunpang, P., Laosuwan, T. (2020) The relationship between normalized difference vegetation index and canopy temperature that affects the **U**rban **H**eat **I**sland phenomenon. *Geographia Technica*, **15**(2), 222-234. http://dx.doi.org/10.21163/GT_2020.152.21

Retnowati, WD., Nurmandi, A., Zahra, AA. (2022). Handling COVID-19 in the capital city of Jakarta with innovation policy: the scale of social restrictions policy. *Heliyon*, **8**(1): e09467. doi: 10.1016/j.heliyon. 2022.e09467

Sajadi MM, Habibzadeh P, Vintzileos A, Shokouhi S, Miralles-Wilhelm F, Amoroso A. (2020). Temperature, Humidity, and Latitude Analysis to Estimate Potential Spread and Seasonality of Coronavirus Disease 2019 (COVID-19). *JAMA Netw Open*. 1;**3**(6): e2011834. doi: 10.1001/jamanetworkopen.2020.11834. PMID: 32525550; PMCID: PMC7290414.

Saputra, A., Hairy, MH, Shofirun S, Saifuddin, A, Furoida, K. (2022). Assessing urban heat island in Jakarta, Indonesia during the pandemic of Covid-19. *IOP Conf. Series: Earth and Environmental Science*, 012069. doi:10.1088/1755-1315/986/1/012069

Schwarz, N; Lautenbach, S; Seppelt, R. (2011). Exploring indicators for quantifying surface urban heat islands of European Cities with MODIS land surface temperatures. *Remote Sensing Environment*, **115**,3175-3186.

Shofirun S; Yusoff, MN; Talib, A; Rahman MAA; Sohaimi, NS; Mokthsim, N; Ibrahim, MH; Saputra, A. (2023). The use of energy in Malaysia: Mapping energy flow from primary source to end use. Proceeding of International Summit on Education, Technology, and Humanity 2021, *AIP Conf. Proc.* 2727, 050028-1–050028-11; https://doi.org/10.1063/5.0141394

Sobrino, J., Jimenez, JC., Paolini, L. (2004). Land surface temperature retrieval from LANDSAT TM 5. *Remote Sensing of Environment*, **90**(4):434-440. doi: 10.1016/j.rse.2004.02.003

Steeneveld, G., Koopmans, S., Heusinkveld, B., Van Hove, L., Holtslag, A. (2011) Quantifying urban heat island effects and human comfort for cities of variable size and urban morphology in the Netherlands, *J. Geophys. Res.: Atmos.*, **116** (D20).

Streutker, D.R. (2003). Satellite-measured growth of the urban heat island of Houston, Texas. *Remote Sensing Environment*, **85**, 282-289.

Sun N, Wei L, Shi S, Jiao D, Song R, Ma L, Wang H, Wang C, Wang Z, You Y, Liu S, Wang H. A. (2020). Qualitative study on the psychological experience of caregivers of COVID-19 patients. *Am J Infect Contro*, **48**(6):592-598. doi: 10.1016/j.ajic.2020.03.018. Epub 2020 Apr 8. PMID: 32334904; PMCID: PMC7141468.

Synnefa, A., Dandou, A., Santamouris, M., Tombrou, M., & Soulakellis, N. (2008). On the use of cool materials as a heat island mitigation strategy. *Journal of Applied Meteorology and Climatology*, **47**(11), 2846-2856.

Taki, HM. And Maatouk, MMH. (2018). Spatial Statistical Analysis for Potential Transit Oriented Development (TOD) in Jakarta Metropolitan Region. *JGEET*, **3**(1). Doi: 10.24273/jgeet.2018.3.01.1091

Tomlinson, C., Chapman, L., Thornes, J., Bakeret, C.J. (2012). Derivation of Birmingham's summer surface urban heat island from MODIS satellite images. *International Journal Climatology*, **32**, 214-224

Wang, K., Aktas YD., Stocker, J., Carruthers, D., Hunt, J., Malki-Epshtein, L. (2019). Urban heat island modelling of a tropical city: case of Kuala Lumpur. *Geosci. Lett.*, **6**:4 https://doi.org/10.1186/s40562-019-0134-2

Wang W, Tang JM, Wei FQ. (2020). Updated understanding of the outbreak of 2019 novel coronavirus (2019-nCoV) in Wuhan, China. *J Med Virol*. https://doi.org/10.1002/jmv.25689

Weng, Q.A. (2001) Remote sensing? GIS evaluation of urban expansion and its impact on surface temperature in the Zhuijang Delta, China. *International Journal of Remote Sensing*, **22**, 1999-2014.

Weng , Q. Lu, D., Schubring, J. (2004) Estimation of land surface temperature-vegetation abundance relationship for urban heat island studies. *Remote Sensing Environment*, **89**, 467-483.

Worachairungreung, M., Thanakunwutthirot., K., Kulpanich, N. (2023). A study on oil palm classification for Ranong province using data fusion and machine learning algorithms. *Geographia Technica*, **18**(1), 161-176. http://dx.doi.org/10.21163/GT_2023.181.12

Yamamoto, Y. (2006). Measures to mitigate urban heat islands. *Science and Technology Trends Quarterly Review*, **18**(1), 65- 83.

Yusof, Amir. (2021) Timeline: How the COVID-19 pandemic has unfolded in Malaysia since January 2020. Mediacrop. https://www.channelnewsasia.com/asia/timeline-how-covid-19-pandemic-has-unfolded-malaysia-january-2020-2082081. Accessed 2 Januray 2024.

Zha, Y., Gao, J., and Ni, S. (2003) Use of normalized difference built-up index in automatically mapping urban areas from TM Imagery. *International Journal of Remote Sensing*, **24**, 583-594.